

# Effect of Temperature on the Liquid Bridging Force while Maintaining Physical Stability in Solid–Liquid Mixed Fuel

Chi Zhang,\* Hangyuan Ma, Jiafan Ren, Ge Song, Yicun Zhao, and Chunhua Bai

Cite This: *ACS Omega* 2024, 9, 19669–19678

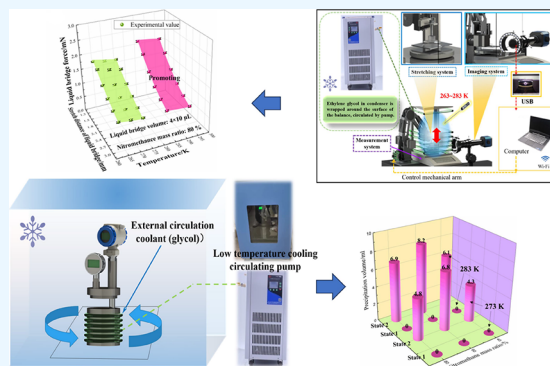
Read Online

ACCESS |

Metrics & More

Article Recommendations

**ABSTRACT:** The temperature factor is an important factor affecting the intercomponent forces while maintaining the physical stability of solid–liquid mixed fuels. Through self-designed experimental equipment, feedback was provided on the fuel stratification and density distribution uniformity with solid–liquid volume ratios of 1.25:1 and 1:1 under different temperature conditions. As the viscosity of the liquid increased with decreasing temperature, the ability of the fuel to overcome particle deposition was enhanced. Although none of the three fuel ratios with a solid–liquid volume ratio of 1.25:1 showed stratification, the differences in the liquid bridging forces of the components resulted in an increasingly uneven distribution of density with increasing surface tension of the liquid components. By analyzing the imaging results and measuring the liquid bridge force, it was found that the fuel with a nitromethane mass ratio of 40% had the lowest temperature effect on the solid–liquid contact area and the most uniform density distribution. Properly reducing the surface tension of liquid components could effectively resist the influence of the temperature on the liquid bridge force while maintaining the physical stability of the fuel.



## 1. INTRODUCTION

The United States proposed the concept of liquid–solid hybrid fuel with liquid as the continuous phase during the development of the fuel–air explosive (FAE) in the 1960s. However, although the fuel performance has significantly improved, the instability caused by solid fuel deposition seriously affects the quality of the product.

To solve the above problem, scholars<sup>1</sup> tried to change the continuous phase of the fuel to a gel shape. Although this practice solved the problem of sedimentation, the poor dispersion effect of the fuel directly led to a sharp reduction in the explosion characteristics. In recent years, many research results have been reported to improve the poor physical stability of liquid–solid fuels. The most common approach is to add certain additives without affecting the final combustion and explosion characteristics. Geller et al.<sup>2</sup> found that after optimizing the formulation of 100% biofuels using diesel, the sediment mass decreased significantly from 15% of the total mass ratio. Zhao and Liu<sup>3</sup> added a small amount of nitrocellulose as a tackifier to propylene oxide–aluminum powder fuel, and the results showed that the sedimentation rate of aluminum powder was effectively suppressed. Wu<sup>4</sup> indicated that when an additive was added to the original liquid–solid FAE at a mass ratio of 3%, the settling time of spherical aluminum powder was significantly prolonged. A common issue of the above methods is that the additives effectively reduce the sedimentation of solid components, but

the physical stability of liquid–solid fuels has not been completely solved.

Flame propagation or explosion overpressure is an important indicator for evaluating fuel reactions.<sup>5–9</sup> Problems with physical stability will result in a decrease in the reaction efficiency of the fuel. To effectively improve the physical stability of fuel, Bai and co-workers<sup>10–12</sup> adjusted the volume ratio of components and proposed the concept of solid–liquid mixed fuel with solid components as continuous phases. Zhang et al.<sup>13–15</sup> determined from the microscopic structural and stacking characteristics of fuel determined that the saturation of liquid fuel filled between fuel pores plays an important role in the physical stability of the fuel. In theory, the phenomenon of liquid–solid stratification occurs only when the fuel is in a liquid supersaturated state. Chen<sup>16</sup> and Hu<sup>17</sup> considered the impact of oscillation on the physical stability of fuel and used the HT-P vertical frequency modulation vibration table as the experimental carrier, combined with the multiphase flow model of fluid dynamics software, to detect the physical

Received: February 29, 2024

Revised: April 9, 2024

Accepted: April 10, 2024

Published: April 22, 2024



stability of different proportions of mixed fuels (epoxy propane/aluminum powder, *n*-pentane/aluminum powder, *n*-hexane/aluminum powder, etc.) under a series of vibration frequency gradients. The results indicated that the air gap filling rate of the solid particle gaps was influenced by the encapsulation ability of liquid fuel on aluminum powder during the charging stage. A lower gap-filling rate and smaller particle spacing resulted in a smaller influence of the oscillation load on the dense distribution of the mixed fuel.

According to previous research results,<sup>18</sup> the liquid bridge force is tens or dozens of times higher than the intermolecular force. If solid particles are hydrophilic and form a liquid bridge between particles, then the liquid bridge force becomes the main influencing factor determining the physical stability of the fuel. You et al.<sup>19</sup> studied the effect of moisture content on particle size during the iron powder granulation process using a horizontal high-shear granulator. The results indicate that as the water content increases, the liquid bridging force increases, leading to an increase in the bonding number of small particles and an increase in the particle size. Pepin et al.<sup>20</sup> conducted a detailed analysis of the liquid bridge force between solid and liquid by adjusting the liquid viscosity and surface tension with hydroxypropyl methyl cellulose and polyethylene pyrrolidone. Their results demonstrate that the liquid bridge force plays a major role in the agglomeration of powders, and the factors affecting the liquid bridge force are mainly the combined effects of liquid surface tension, the Laplace pressure of the liquid bridge, and liquid viscosity. It has been proven that the viscosity and surface tension characteristics of liquids are influenced by temperature, and strict requirements have been promoted for the physical stability of solid–liquid mixed fuels at different temperatures due to fuel adaptability considerations.

To clarify the influences of temperature factors on the physical stability of solid–liquid mixed fuels, flake aluminum powder mixed with liquid fuels diethyl ether and nitromethane is selected, and corresponding detection devices are designed to investigate the liquid precipitation and density distribution characteristics of the fuel at different temperatures. Based on the trend in results under the influence of temperature factors, the role of the liquid bridge force in maintaining the physical stability of mixed fuel is clarified. The law of liquid bridge force under the influence of temperature factors can serve as an important variable factor, providing a valuable reference for the final integration of models that can evaluate the physical stability of solid–liquid mixed fuels.

## 2. EXPERIMENTAL METHODS

### 2.1. Physical Stability Detection Device and the Experimental Group.

The liquid fuels used in this experiment are analytical-grade ether (purity of 99.5%) and analytical-grade nitromethane (purity of 99%). The median particle size of aluminum powder is 14.28  $\mu\text{m}$ ,<sup>21</sup> with a bulk stacking density of 400 kg/m<sup>3</sup>. Due to the detailed introduction of the experimental system for the physical stability of fuel at 293 K in previous studies,<sup>11</sup> only a brief introduction is provided here. The top of the container is connected to a pressure gauge (measuring range of 0–60 kPa, accuracy level of 0.25%, and sampling frequency of 3 times/second) and a thermometer (measuring error of  $\pm 0.4$  K). After premixing the fuel according to the solid–liquid ratio and nitromethane mass ratio shown in Table 1, oscillation experiments are conducted in the container. In the

**Table 1. Grouping of Solid–Liquid Mixed Fuel Stability Experiments**

group abbreviation	abbreviation	solid–liquid ratio	mass ratio of nitromethane in liquid components/%	ambient temperature/K
80% group	state 1	1.25:1	80	283
	state 2	1:1	80	
60% group	state 1	1.25:1	60	273
	state 2	1:1	60	
40% group	state 1	1.25:1	40	263
	state 2	1:1	40	

experimental part of fuel physical stability in different temperature environments, the device accelerates fuel stratification by applying a certain frequency of oscillation, with a constant oscillation frequency of 120 rpm and an oscillation time of 4 h. The surface of the container is wrapped with a hose filled with ethylene glycol condensate, and the cooling circulation pump is responsible for the circulation of the cooling system. The experimental temperature is controlled between approximately 263 and 283 K. As shown in Figure 1 A

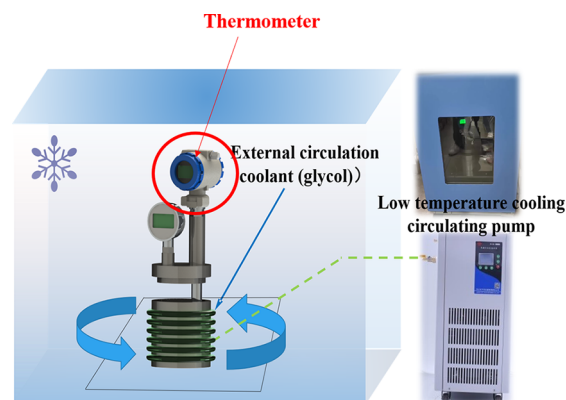


**Figure 1.** Experimental Assembly for the Physical Stability of solid–liquid mixed fuel in different temperature environments.

thermometer was inserted into the container to monitor temperature changes in real-time. During the oscillation process, the temperature change does not exceed 0.2 K and would not affect the experimental results. After the fuel oscillation is completed, the height H1 of the fuel stack inside the container is measured and then the height H2 of the fuel stack after using a needle to remove the precipitated liquid is measured. Subsequently, the top, middle, and bottom densities are calculated by dividing the fuel into three equal parts according to the value H1. The top fuel includes the precipitated liquid fuel and the remaining solid–liquid mixed fuel with a stacking height of  $H2 - H1/3$ .

### 2.2. Experimental Assembly and Grouping of Liquid Bridge Forces.

The experimental assembly is shown in Figure 2, where the main body consists of an imaging system, a liquid bridge stretching system, a liquid bridge force measurement system, and a temperature control system. The experimental principle is shown in Figure 3. The robotic arm operates through the control of the program, and the changes in the morphology of the liquid bridge are captured by a horizontal microscope (GP-50, GAOPIN, China) and transmitted in real time to the analysis system (S-EYE) through a USB connection. The measurement system is an electronic balance

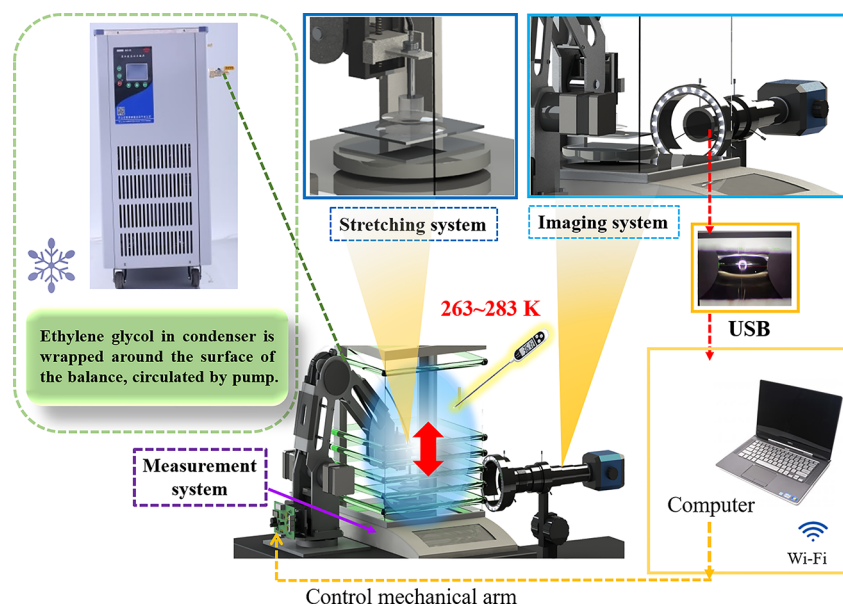


Figure 2. Liquid fuel bridge force experimental device.

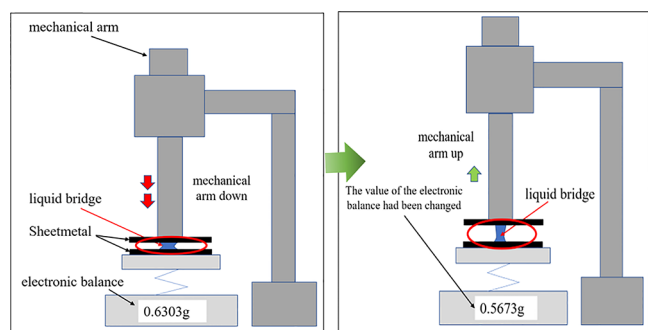


Figure 3. Principle of the liquid fuel bridge force experimental device.

with an accuracy of 0.1 mg. When the metal surface contacts a liquid droplet and forms a liquid bridge, the reading of the balance changes accordingly. The liquid bridge force  $F_{lb}$  at this time can be calculated using formula 1:<sup>22,23</sup>

$$F_{lb} = (m_{dry} - m_{wet})g \quad (1)$$

where  $m_{dry}$  is the reading of the balance when the liquid bridge is not formed (the metal plate is not in contact with the liquid droplet),  $m_{wet}$  is the reading of the balance when the liquid bridge is formed, and  $g$  is the local gravitational acceleration. The length, contact diameter with the metal plate, contact angle, and other parameters during the stretching process of

the liquid bridge can be directly measured using the above software.

In the process of fuel mixing, the liquid components may not exist in a complete single liquid bridge form due to pressure or surface tension factors when solid particles penetrate a certain volume of liquid fuel. This part of the liquid either forms multiple independent and small single liquid bridges due to the presence of bubbles or contacts the surrounding solid components in a form similar to multiple liquid bridges. The contact area between the liquid bridge and the solid and the surface tension and pressure difference of the liquid bridge undergo certain changes relative to the form of a single liquid bridge. Therefore, as shown in Table 2, representative liquid bridge volumes of  $4 \times 5$  and  $4 \times 10 \mu\text{L}$  are directly selected for the experimental detection of the variation in the combined forces of multiple liquid bridges with tensile height at different temperatures for two liquid ratios (nitromethane mass ratios of 80 and 40%) with significant surface tension differences. The solid metal is an aluminum plate.

The grouping of liquid bridge force experiments is shown in Table 1, where the multiliquid bridge experiment splits the volume into  $4 \times 5$  and  $4 \times 10 \mu\text{L}$  (4 small liquid bridges with equal volume). In addition, considering that liquid fuel fills the limited gaps between particles in actual products, the spacing between the four equal volume liquid bridges is strictly controlled within a limited range.

Table 2. Grouping of Liquid Bridge Force Experiments

factors	mass ratio of nitromethane in liquid fuel/%	volume of liquid fuel/ $\mu\text{L}$	surface tension of mixed solution (20 °C)/mN/m	ambient temperature/K	metal plate
liquid fuel volume	60	$4 \times 5$	29.64	283	magnesium aluminum
		20			
		$4 \times 10$			
		40			
liquid fuel surface tension	80	$4 \times 5$	33.77	268	
		20			
		$4 \times 10$			
		40			
	40	$4 \times 10$	26.36	263	

**2.3. Experimental System Accuracy and Error Analysis.** The literature referenced in this system is based on a large amount of experimental data and is combined with previous semiempirical formulas for the liquid bridge force between two spherical surfaces. The liquid bridge force formula is corrected and obtained for different liquid bridge morphologies between two parallel surfaces, and the relationship between the liquid bridge force and various parameters meets the relationship shown in formula 2. To verify the accuracy of the experimental system designed based on this experimental principle, volumes ranging from 20 to 50  $\mu\text{L}$  of nitromethane are selected to investigate the liquid bridge force between metal aluminum plates, and the experimental values obtained are compared with the theoretical values derived from formula 2. The parameters needed for theoretical value derivation are shown in Figure 4, which can be directly measured by using S-EYE software.

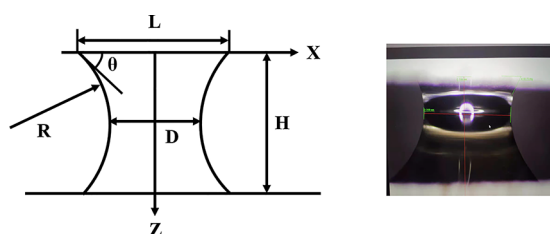


Figure 4. Schematic diagram of liquid bridge-related parameters.

The liquid bridge force acting between two planes is jointly affected by two factors, one of which is the pressure difference between the inside and outside of the liquid surface bending part,  $\Delta P$ . The other part is through the vertical component of surface tension along the tangent direction of the meniscus.

$$F = \pi \left( \frac{L}{2} \right)^2 \Delta P + \pi L \cdot \gamma \cdot \sin\theta \quad (2)$$

where  $L$  is the diameter of the contact part between the liquid fuel and the metal sheet,  $\gamma$  is the surface tension coefficient of the liquid, and  $\Delta P$  is the internal and external pressure difference at the gas–liquid two-phase interface. When the liquid bridge remains stable, formula 3 is valid:

$$\Delta P = \gamma \left( \frac{1}{r_1} + \frac{1}{r_2} \right) \quad (3)$$

where parameters  $r_1$  and  $r_2$  represent the two main curvature radii of the gas–liquid interface of the liquid bridge, respectively. To ignore gravity, the meniscus can be approximated as an arc. Therefore, by solving the Young Laplace differential equation,  $r_1 = R$  and  $r_2 = -D/2$  can be obtained. After transformation, the following geometric relationship can be obtained:

$$R = \frac{H}{2\cos\theta} \quad (4)$$

$$L = D + 2R(1 - \sin\theta) \quad (5)$$

where  $H$  is the height of the liquid bridge,  $D$  is the minimum diameter of the neck of the liquid bridge, and  $\theta$  is the contact angle between the liquid bridge and the parallel metal sheet. The above parameters can be directly measured through the software. Figure 5 shows a comparison between the actual

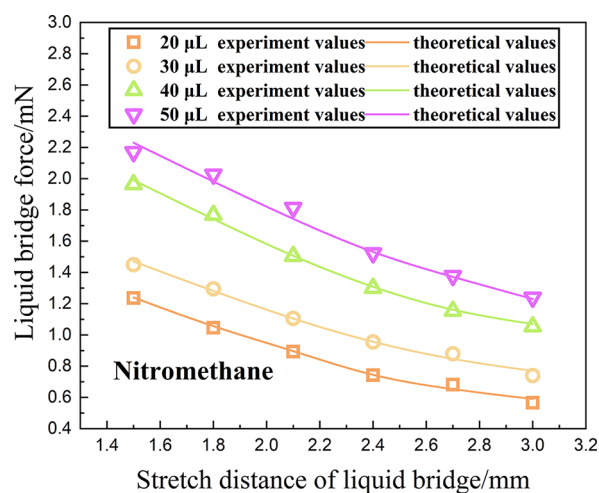


Figure 5. Actual and theoretical formula values of the liquid bridge force.

values of the nitromethane liquid bridging force and theoretical values derived from formula 1, where the theoretical values are represented by solid lines, and the actual values are represented by points. The comparison results are shown in the figure, and the vast majority of points representing actual measured values fall on the curve representing theoretical values. The maximum error between the actual value and the theoretical value is 6.1%, and there are two reasons for the error. First, the theoretical formula is derived from two smooth and parallel planes, but the actual metal sheet has a certain roughness (1.6–3.2  $\mu\text{m}$ ). Conversely, the theoretical formula uses an approximate solution method in the derivation process, resulting in a slight error in the curvature radius relative to the actual curved liquid surface. The results indicate that in the process of characterizing the liquid bridge force between the solid and liquid phases in this article, a certain error exists between the actual value and the theoretical value, but it does not affect the accuracy of the experimental equipment detection results.

### 3. RESULTS AND DISCUSSION

Figure 6 shows the volume of liquid fuel precipitation after 4 h of oscillation at 120 rpm for solid–liquid volume ratios of 1:1 and 1.25:1 at ambient temperatures of 263–283 K. For fuels with the same solid–liquid ratio, there is no stratification in state 1 fuel, while state 2 fuel shows a trend of liquid precipitation decreasing with decreasing ambient temperature. Previous research results have shown that fuel with a solid–liquid volume ratio of 1:1 may have two stages during the stratification process.<sup>11</sup> In the first stage, the solid components suspended in the liquid precipitate within half an hour and a large amount of liquid fuel floats on top. Continuously oscillating the lower sediment layer results in a small amount of liquid fuel appearing in the second stage. The particles in the first stage are suspended in the liquid, and the main obstacle to stratification is the internal friction force (liquid viscosity) between the liquid and the liquid. The viscosity of the liquid increases with decreasing ambient temperature, which enhances the anti-settling ability of the state 2 mixed fuel.

In addition, by observing the volume of liquid precipitates between the 80 and 40% groups under various temperature conditions, it is found that when the ambient temperature drops to 263 K, there is no significant difference in the volume

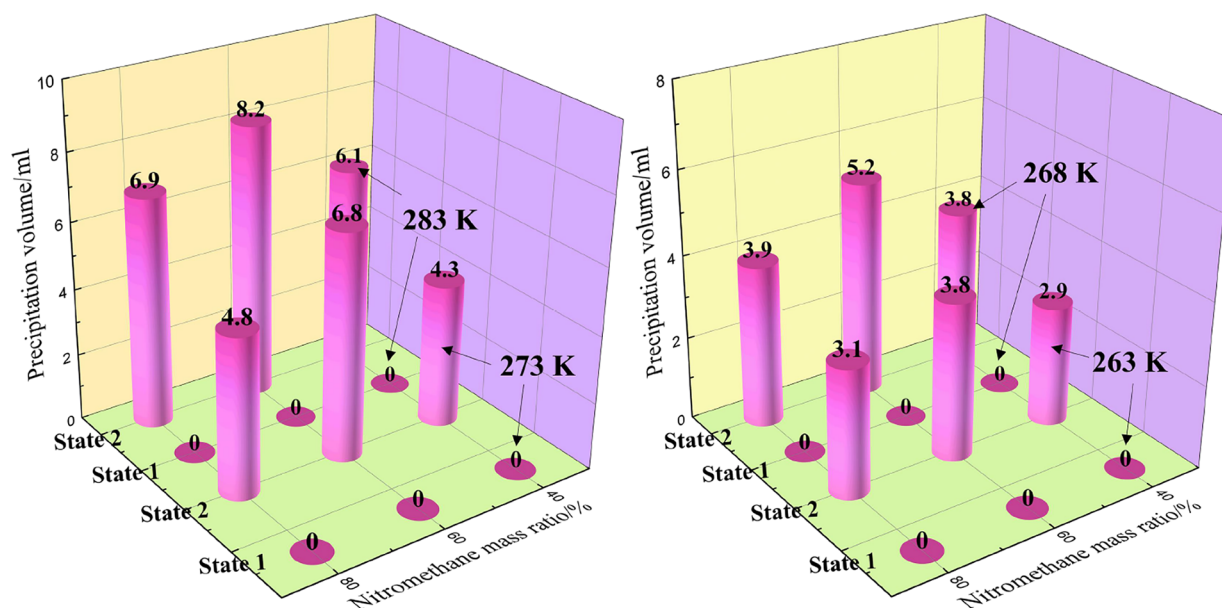


Figure 6. Liquid precipitation volume at temperatures of 263–283 K (oscillation frequency of 120 rpm and oscillation time of 4 h).

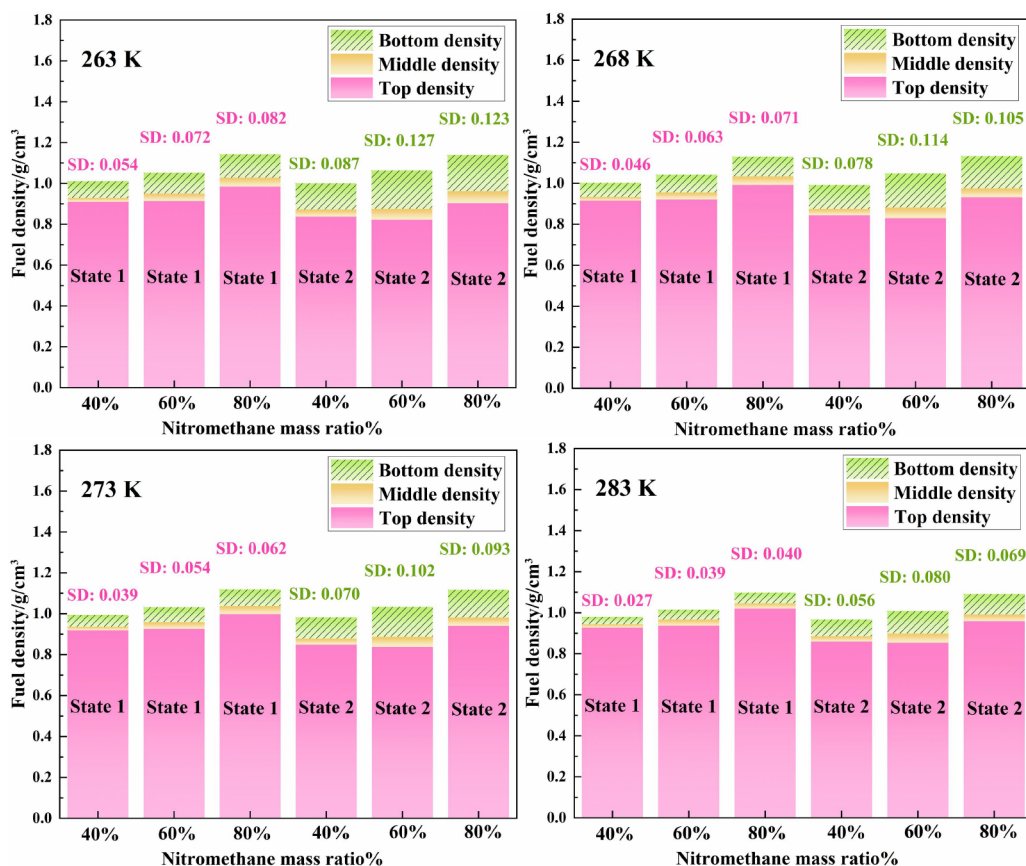
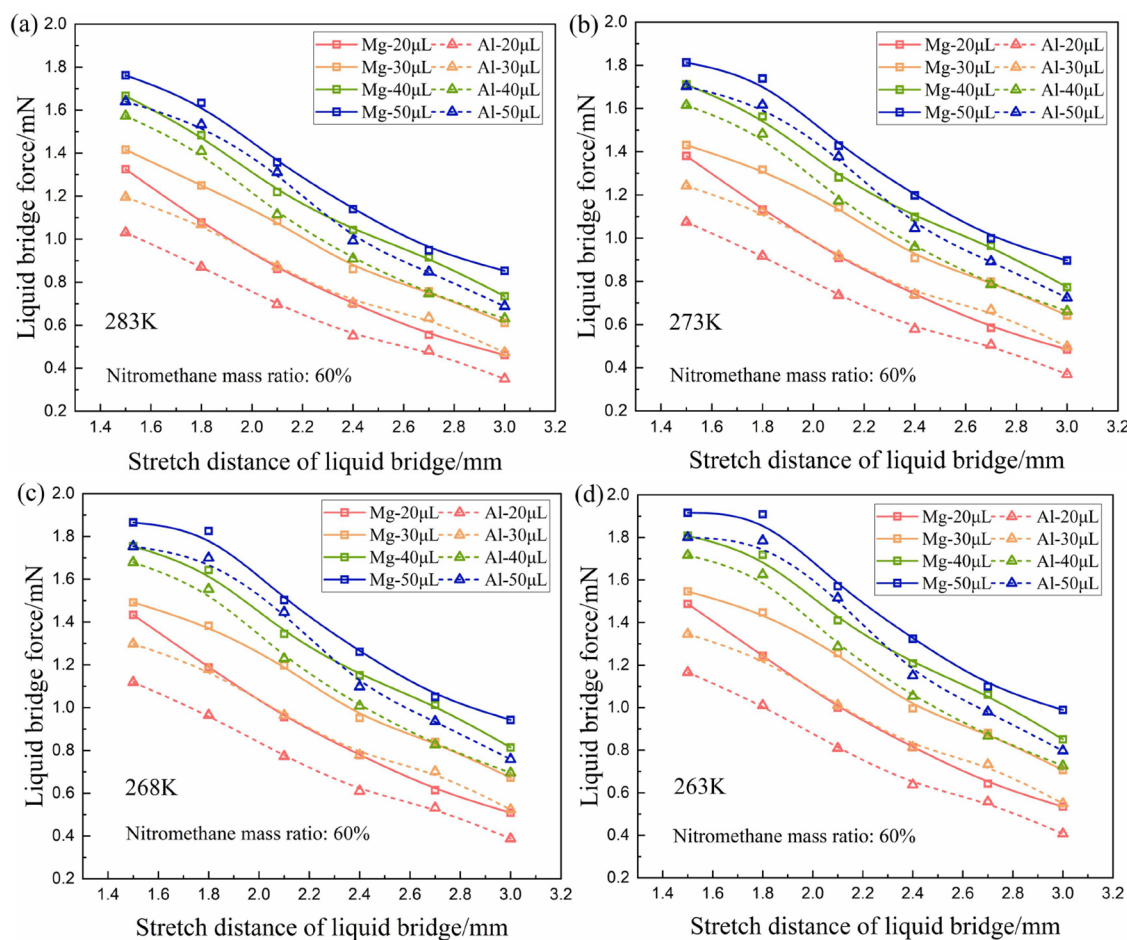


Figure 7. Fuel density distribution trend at temperatures of 263–283 K (oscillation frequency of 120 rpm, oscillation time of 4 h, and SDs of the top, middle, and bottom fuel densities; State1: 1.25:1, State2: 1:1).

of liquid precipitates in this environment. According to the chemical manual,<sup>24</sup> the viscosity of nitromethane is 0.648 mPa·s (293 K), and the viscosity of liquid ether is 0.225 mPa·s (293 K). The viscosity of the mixed liquid fuel decreases with the decrease in the proportion of nitromethane in the component. This finding indicates that for fluid fuels, the significant increase in liquid viscosity while reducing ambient temperature

greatly enhances their anti-settling ability. In the above process, the increase in the viscosity of the liquid becomes an important factor in resisting the first-order stratification of the fuel.

The most fatal damage to products caused by the precipitation of liquid fuel is the weakening of the uniformity of the density distribution, which directly leads to the inability of the fuel to achieve the desired usage effect. Figure 7



**Figure 8.** Liquid bridge volume factors on liquid bridge forces under different temperatures (a. 283 K, b. 273 K, c. 268 K, d. 263 K; solid line: experimental results of metal magnesium plate and dashed line: metal aluminum plate).

corresponds to the density distribution results of the fuel with three liquid distribution ratios under two solid–liquid volume ratios of 1.25:1 and 1:1 at temperatures of 263, 268, 273, and 283 K, respectively, after oscillation at 120 rpm for 4 h. As the temperature decreases, the density of the mixed fuel increases from top to bottom under all conditions. To intuitively determine the uniformity of the fuel, a dimensionless criterion is introduced to perform a standard deviation analysis on the density of the three parts of the fuel. The standard deviation (SD) value of the density of the three parts of fuel with the same ratio shows an increasing trend. The results indicate that for fuels with the same liquid component distribution ratio (nitromethane mass ratio), the fuel density uniformity of the solid–liquid volume ratio of 1.25:1 is much better than that of the solid–liquid volume ratio of 1:1.

Another aspect that needs to be taken seriously is that although the group with a solid–liquid volume ratio of 1.25:1 does not exhibit stratification, there is a phenomenon of top density < middle density < bottom density under oscillation conditions. For mixed fuels with different solid–liquid ratios, the trend of fuel stability varies as the mass ratio of nitromethane in the liquid component increases. For the State 1 group, the standard deviation (SD) value of the fuel density distribution shows a decreasing trend, while for the State 2 group with stratification, the SD values of the three liquid ratios show a trend of first increasing and then decreasing; that is, the fuel stability is 40% group >80%

group >60% group. Therefore, when determining the uniformity of fuel density in different temperature environments, it is necessary to consider both stratification factors and focus on analyzing the solid–liquid interaction forces of the mixed fuel.

According to previous research results,<sup>11,18</sup> the liquid bridge force plays an important role in maintaining the physical stability of the fuel. The results obtained at 293 K indicate that the liquid bridge force can be influenced by both the volume of the liquid bridge and the surface tension. Figure 8a–d corresponds to the variation in the liquid bridge force with different liquid bridge volumes and stretching heights (from 1.5 to 3 mm) under four temperature conditions of 263–283 K. Under these temperature conditions, there are no differences in the change trends of the liquid bridge force relative to the trend at 293 K. As the stretching height increases, the liquid bridge force gradually decreases, and larger-volume liquid bridges have greater liquid bridge forces.

As the temperature decreases, the liquid bridge force at each stretching height increases to a small extent. The maximum liquid bridge force is observed at a temperature of 263 K and a stretching height of 1.5 mm. The change in temperature mainly affects the physical properties of the liquid fuels. For solid–liquid mixed fuels with the same liquid fuel ratio, viscosity plays a dominant role in affecting physical stability. In addition, under the same temperature conditions, the decrease in liquid bridge force (the height of the liquid bridge is

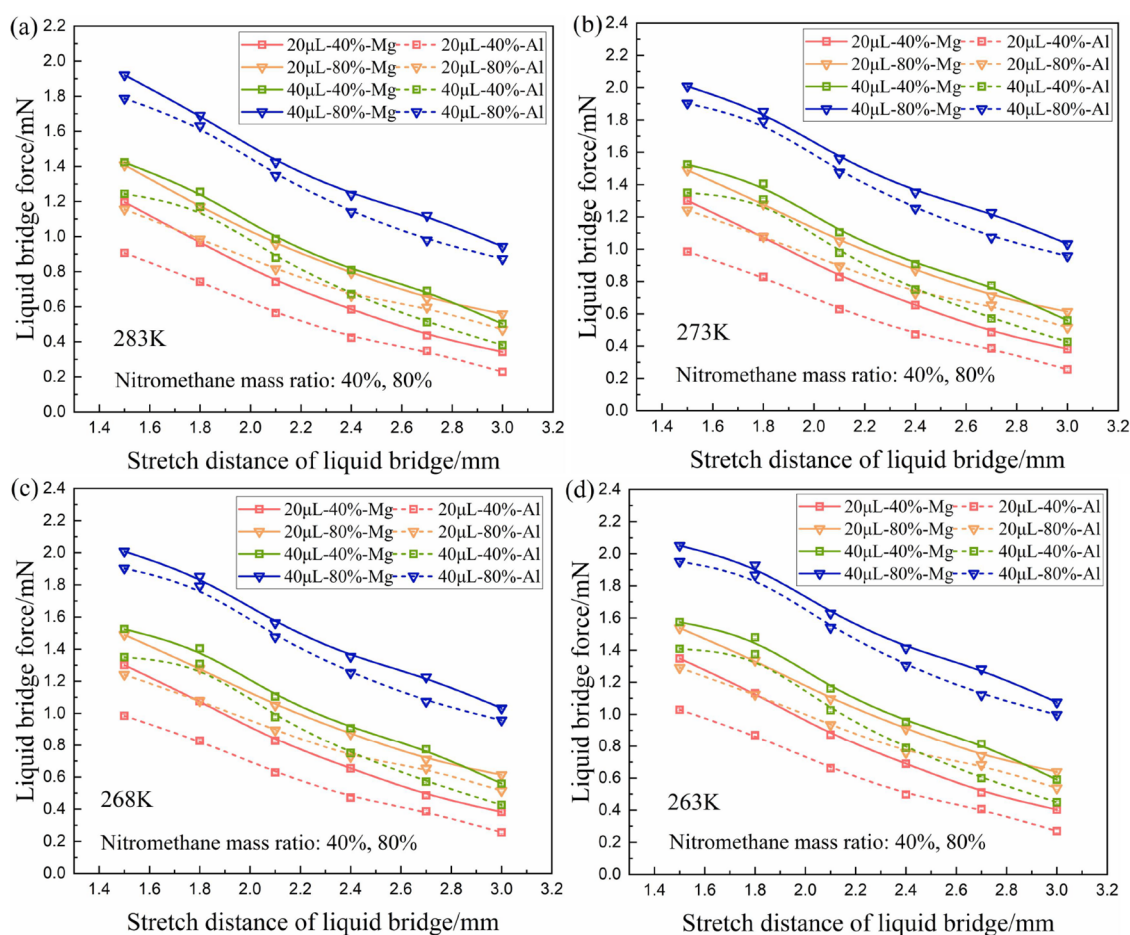


**Figure 9.** Liquid surface tension factors on liquid bridge forces at different temperatures (a. 283 K; b. 273 K; c. 268 K; d. 263 K; solid line: experimental results of metal magnesium plate; dashed line: metal aluminum plate).

stretched from 1.5 to 3 mm) shows a decreasing trend as the volume of the liquid bridge increases, and the decrease in amplitude slows with the decrease in ambient temperature. By taking the experimental results of magnesium plates in Figure 8d as an example, at a temperature of 263 K, the volume is between 20 and 50  $\mu\text{L}$ . The decreases are 63.9, 54.3, 52.9, and 48.3%, respectively, which are slightly lower than the decreases of 65.1, 56.8, 55.9, and 51.6% at 283 K.

Figure 9a–d shows the variations in the liquid bridge force under different stretching conditions for liquid bridges with mass ratios of 80 and 40% of nitromethane at temperatures ranging from 263 to 283 K. Under the conditions of 263–268 K, when the volume of the liquid bridge is constant, the liquid bridge force decreases with the decrease in the surface tension of the liquid component. The 80% group with higher liquid surface tension always maintains a higher liquid bridge force than the 40% group. As the temperature decreases, the liquid bridge force increases slightly under all conditions, but there is no significant difference in the enhancement between the 80% group and the 40% group.

At 283 K, by measuring the volume of the mixed fuel with the same solid-to-liquid ratio (1.25:1), it is found that the volumes of the 80% group, 60% group, and 40% group after mixing are 62, 60, and 58  $\text{cm}^3$ , respectively. This trend, combined with the results of liquid bridge force experiments, indicates that the filling saturation of liquid fuel in the solid–liquid gap is closely related to its surface tension. Conversely, components with high interstitial saturation are filled with large

volumes of liquid bridges, resulting in strong intermolecular forces and high physical stability. For solid–liquid mixed fuels with different liquid fuel ratios, temperature factors will affect the volume of liquid bridges between solid components. The difference in liquid bridging forces between components will directly dominate the physical stability of the fuel.

The surface shown in Figure 10a–d is obtained through fitting based on the stretching heights of multiple liquid bridge groups and through setting the temperature as the independent variable and the experimentally measured liquid bridge force as the dependent variable. Several interesting results are found by comparing the experimental values of the multiliquid bridge force in Figure 10 with the single liquid bridge force in Figure 9. Figure 10a,b shows the variations in the liquid bridge force with stretching height and temperature when the liquid ratio (nitromethane mass ratio) is 80 and 40%, respectively, for a multiliquid bridge with a liquid bridge composition of  $4 \times 5 \mu\text{L}$ . In the figure, the red dots that do not fall on the plane indicate that the liquid bridge is broken at this time. By comparing the conclusion of this experiment with the previously obtained single liquid bridge force under the same conditions, there is no significant difference in the combined force of multiple liquid bridges between the  $4 \times 5 \mu\text{L}$  groups relative to the single liquid bridge group.

In addition, at a temperature of 293 K, the multiliquid bridge with a  $4 \times 5 \mu\text{L}$  morphology in the 80% group should have reached the critical tensile height at 2.7 mm, but no liquid bridge fracture is observed when the temperature is set to 268

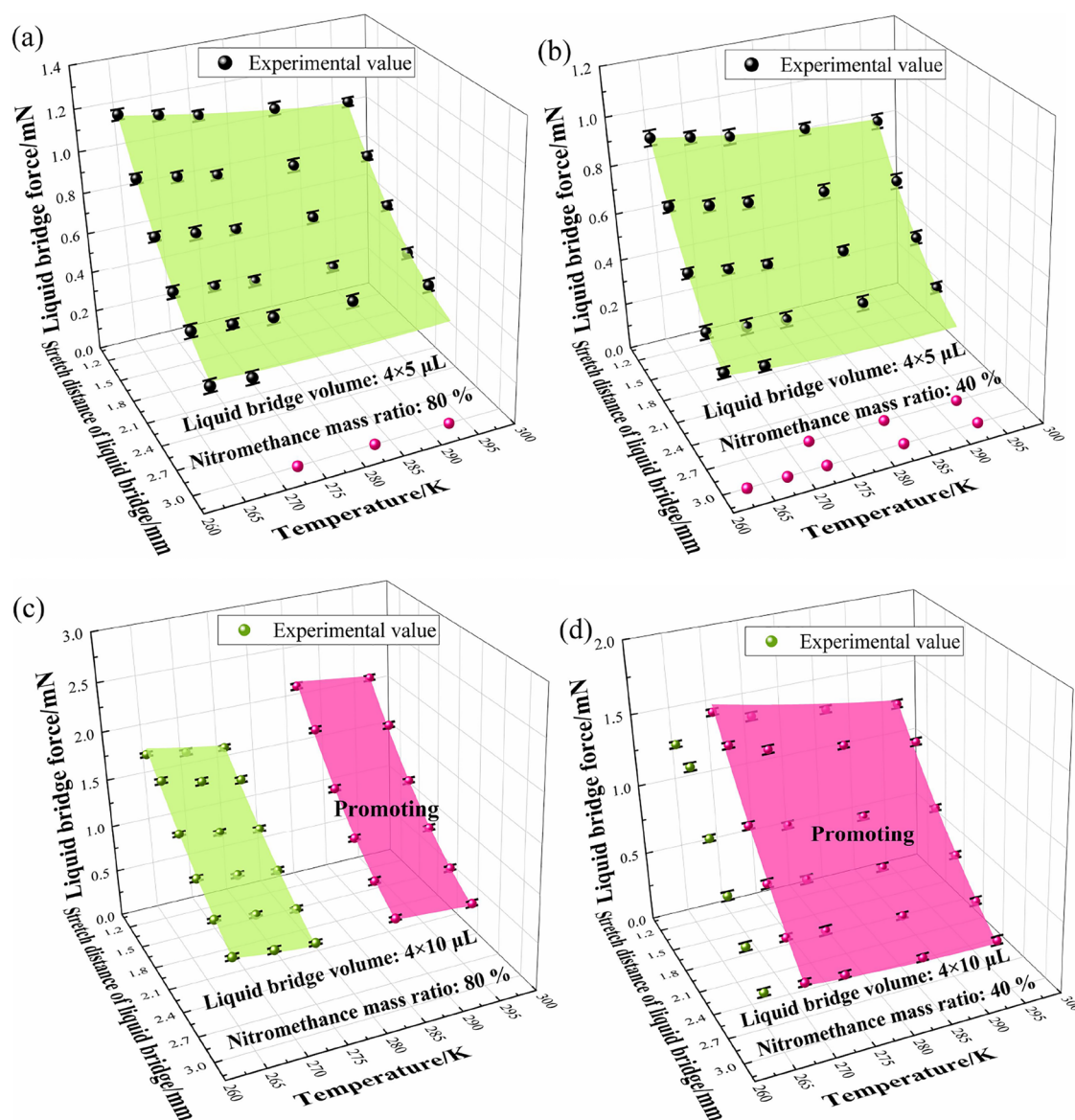


**Figure 10.** Combined force generated by multiple liquid bridges at different environmental temperatures (a. Liquid volume  $4 \times 5 \mu\text{L}$ , Nitromethane mass ratio 80%; b. Liquid volume  $4 \times 5 \mu\text{L}$ , Nitromethane mass ratio 40%; c. Liquid volume  $4 \times 10 \mu\text{L}$ , Nitromethane mass ratio 80%; d. Liquid volume  $4 \times 10 \mu\text{L}$ , Nitromethane mass ratio 40%; the points in the figure represent the liquid bridge force measured in the experiment).

K. This finding indicates that as the ambient temperature decreases, the axial tensile resistance of liquid fuel is enhanced. The multiliquid bridge with a liquid bridge composition of  $4 \times 5 \mu\text{L}$  does not produce significantly higher liquid bridge forces than the single liquid bridge group under the same conditions when the liquid ratio (nitromethane mass ratio) is 80 or 40% (the fitted plane is indicated in green).

Figure 10c,d shows the variations in the liquid bridge force with stretching height and temperature when the liquid ratio (nitromethane mass ratio) is 80 and 40%, respectively, for a multiliquid bridge composed of  $4 \times 10 \mu\text{L}$ . No liquid bridge fracture is observed in the  $4 \times 10 \mu\text{L}$  group experiment. At a temperature of 293 K, the combined force generated by the  $4 \times 10 \mu\text{L}$  group with multiple liquid bridges is significantly higher than that of the single liquid bridge group ( $40 \mu\text{L}$  group). At 283 K, two ratios of multiple liquid bridges can produce this result; the liquid bridge combined force generated by the 80% group of multiple liquid bridges at a tensile height

of 1.5 mm is approximately 33% higher than that of the single liquid bridge group. However, 80% of the group first loses the positive effect mentioned above when the ambient temperature drops to 273 K, while the 40% group maintains a higher liquid bridge force than the single liquid bridge group between 11.2 and 17.6% within a stretching height range of 1.5–2.1 mm until the temperature drops to 263 K. The significant increase part is separately fitted, resulting in a red surface that differs from the green surface.

By comparing the morphological changes of the same volume of multiliquid bridge under different temperature conditions during the stretching process, the reasons for the above differences are analyzed. According to the imaging results, in a limited space, a large liquid bridge formed by four relatively independent small liquid bridges and a central wrapping area will be formed, as shown in Figure 11. The volume of the liquid bridge is greater than that of a single liquid bridge under the same conditions. The conclusion

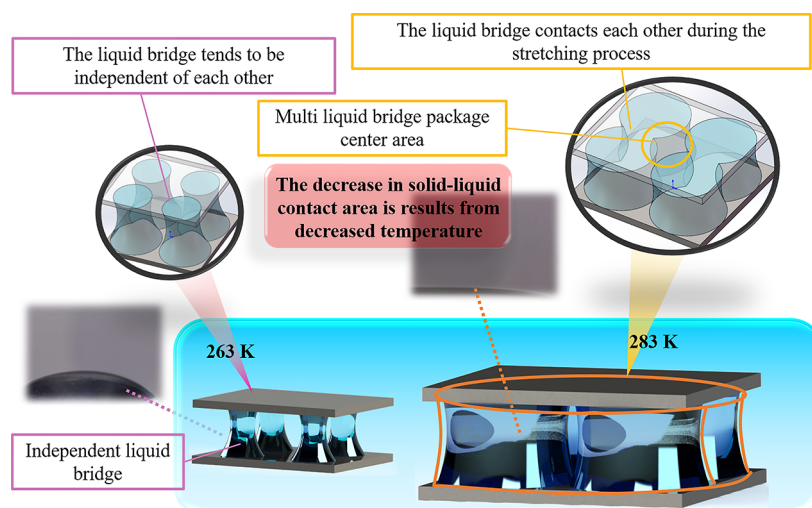


**Figure 11.** Analysis of multiple liquid bridge imaging at different temperatures.

drawn from Figure 9 is that larger liquid bridges generate greater liquid bridge forces between the solid and the liquid phases. As the temperature decreases, the contact area between each small liquid bridge and the solid decreases with decreasing liquid surface tension. The 80% group cannot form a large liquid bridge when the temperature drops to 273 K, resulting in the inability to produce a significantly higher liquid bridge force than that of the control group. The 40% solid–liquid contact area of the group is less affected by temperature factors; thus, it can maintain a high liquid bridge force at an ambient temperature of 268 K. This result indicates the difference in the red areas between the two groups in Figure 10 and indirectly explains the trend of fuel density uniformity in state 1 (solid–liquid volume ratio 1.25:1) in Figure 7 with three liquid group distribution ratios. Higher filling saturation generates greater solid–liquid interaction forces, which can effectively maintain the uniformity of the fuel's physical density. Saturation is another important factor in determining the physical stability of the fuel.

#### 4. CONCLUSIONS

To determine the impacts of temperature factors on the physical stability of solid–liquid mixed fuels, the stratification phenomenon and density distribution uniformity of fuels in different temperature environments are analyzed by using a self-designed device. The conclusions are as follows:

1. Only the mixed fuel with a solid–liquid volume ratio of 1:1 exhibits stratification, and the volume of liquid precipitation decreases with decreasing temperature. This phenomenon may occur because the viscosity of liquid fuel increases with decreasing temperature, thereby enhancing the physical stability of the fuel in the particle settling stage.
2. The fuel with a solid–liquid volume ratio of 1.25:1 is not stratified, but its density uniformity is still affected by oscillation. The group with a mass ratio of 80% nitromethane in the liquid component has the lowest liquid filling saturation, resulting in a relatively small liquid bridging force between the components and poor fuel density uniformity.
3. When the ambient temperature drops from 283 to 263 K, the 40% group with the highest surface tension is the

least affected. The contact area between the multi-liquid bridge and the solid metal plate remains basically unchanged at 273 K, maintaining the existence of the large liquid bridge as much as possible and ensuring the good physical stability of the fuel.

In this study, it is clarified that temperature factors can affect the liquid bridge force, resulting in changes in physical stability. This provides a valuable reference basis for the subsequent research of fuel physical stability.

#### ■ AUTHOR INFORMATION

##### Corresponding Author

Chi Zhang – Beijing Aerospace Propulsion Institute, Beijing 100076, China; [orcid.org/0009-0009-9354-5854](https://orcid.org/0009-0009-9354-5854);  
Email: [zhangc920101703@163.com](mailto:zhangc920101703@163.com)

##### Authors

Hangyuan Ma – Beijing Aerospace Propulsion Institute, Beijing 100076, China  
Jiafan Ren – State Key Laboratory of Explosion Science and Technology, Beijing Institute of Technology, Beijing 100081, China  
Ge Song – Beijing Aerospace Propulsion Institute, Beijing 100076, China  
Yicun Zhao – Beijing Aerospace Propulsion Institute, Beijing 100076, China  
Chunhua Bai – State Key Laboratory of Explosion Science and Technology, Beijing Institute of Technology, Beijing 100081, China

Complete contact information is available at:  
<https://pubs.acs.org/10.1021/acsomega.4c01904>

##### Notes

The authors declare no competing financial interest.

#### ■ ACKNOWLEDGMENTS

This work is supported by State Key Laboratory of Explosion Science and Technology of Beijing Institute of Technology.

#### ■ REFERENCES

- (1) Bai, C. H.; Liang, H. M.; Li, J. P. *Cloud detonation*; Beijing Science Press: Beijing, 2012.

- (2) Geller, D.; Adams, T.; Goodrum, J.; et al. Storage stability of poultry fat and diesel fuel mixtures: Specific gravity and viscosity. *Fuel* **2008**, *87*, 92–102.
- (3) Zhao, J. S.; Liu, R. H. Study on the Stability of the High Energy Fuel Epoxy Propane Aluminum Powder System for Cloud Explosion Bombs. *Chin. J. Explos. Propellants* **1984**, *5*, 8–14.
- (4) Wu, X. X. *Study of physical and chemical stability of liquid-solid FAE fuels*; Nanjing University of Science and Technology: Nanjing, 2013.
- (5) Zhang, B.; Yang, Z. Z.; Leo, Y. D. On the dynamics of drifting flame front in a confined chamber with airflow disorder in a methane-air mixture. *Fuel* **2024**, *357*, No. 129761.
- (6) Yang, Z. Z.; Cheng, J.; Zhang, B. Deflagration and detonation induced by shock wave focusing at different Mach numbers. *Chinese Journal of Aeronautics* **2024**, *37* (2), 249–258. 2023
- (7) Zhang, B.; Li, Y.; Liu, H. Analysis of the ignition induced by shock wave focusing equipped with conical and hemispherical reflectors. *Combust. Flame* **2022**, *236*, No. 111763.
- (8) Zhang, B.; Liu, H. The effects of large scale perturbation-generating obstacles on the propagation of detonation filled with methane–oxygen mixture. *Combust. Flame* **2017**, *182*, 279–287.
- (9) Zhang, B.; Liu, H.; Wang, C. On the detonation propagation behavior in hydrogen-oxygen mixture under the effect of spiral obstacles. *Int. J. Hydrogen Energy* **2017**, *42*, 21392–21402.
- (10) Liu, W. J.; Bai, C. H.; Liu, Q.; Yao, J.; Zhang, C. Effect of metal dust fuel at a low concentration on explosive/air explosion characteristics. *Combust. Flame* **2020**, *221*, 41–49.
- (11) Zhang, C.; Bai, C. H.; Ren, J. F.; Yao, J. Influence of Liquid Bridge Force on Physical Stability During Fuel Storage and Transportation. *Def. Technol.* **2023**, *29*, 106 DOI: 10.1016/j.dt.2022.10.009.
- (12) Liu, W.; Bai, C. H.; Liu, Q. M.; Yao, J.; Zhang, C. Effect of low-concentration RDX dust on solid–liquid mixed fuel characteristics. *Combust. Flame* **2021**, *225*, 31–38.
- (13) Zhang, Q.; Yan, H.; Bai, C. H. Analysis on the Physical Stability of the Solid-liquid Mixed Fuel. *Chin. J. Explos. Propellants* **2003**, *4*, 47–50.
- (14) Zhang, Q.; Bai, C. H.; Liu, Q. M. Analysis and research on the relationship between the mesostructured and detonation of solid-liquid mixed fuel. *J. Basic Sci. Eng.* **2000**, *1*, 106–110.
- (15) Zhang, Q.; Bai, C. H.; Liu, Q. M. Analysis of Mixed Solid and Liquid Fuel State and Character. *J. Combust Sci. Technol.* **2001**, *3*, 288–290.
- (16) Chen, T. T. *Study on Stability of Solid-Liquid Mixed State FAE Fuel*; Beijing Institute of Technology: Beijing, 2015.
- (17) Hu, H. L. *Study on the physical stability of Solid - liquid mixed Fuel Air Explosive*; Beijing Institute of Technology: Beijing, 2018.
- (18) Zhang, C.; Bai, C. H.; Yao, J. Liquid component effect on the dispersion and explosion characteristics of solid-liquid mixed fuel. *Fuel* **2022**, *319*, No. 123806.
- (19) You, Y.; Guo, J. B.; Li, G.; Lv, X. W.; Wu, S. S.; Li, Y.; Yang, R. Y. Investigation the iron ore fine granulation effects and particle adhesion behavior in a horizontal high-shear granulator. *Powder Technol.* **2021**, *394*, 162–170.
- (20) Pepin, X.; Simons, S. J. R.; Blanchon, S. Hardness of moist agglomerates in relation to interparticle friction, granule liquid content and nature. *Powder Technol.* **2001**, *1–2*, 123–138.
- (21) Yao, J.; Zhang, C.; Liu, W. J.; Bai, C. H.; Zhao, X. Y.; Sun, B. F.; Liu, N. The explosion characteristics of diethyl ether-Al mixtures under different ambient conditions. *Combust. Flame* **2021**, *227*, 162–171.
- (22) Zhou, D. *Research on the heavy drop morphologies on solid surfaces*; Beijing Institute of Technology: Beijing, 2017.
- (23) Lu, Z. P. *Researching of the drop morphologies on solid surface*; Beijing Institute of Technology: Beijing, 2016.
- (24) Xiang, S. G.; Liu, G. Q.; Ma, L. X. *Handbook of Chemical and Chemical Property Data - Organic Volume*; Chemical Industry Press: Beijing, 2013.